

Article

Recovery of Pd(II) Ions from Aqueous Solutions Using Activated Carbon Obtained in a Single-Stage Synthesis from Cherry Seeds

Tomasz Michałek ^{1,*}, Konrad Wojtaszek ¹, Stanisław Małecki ¹, Kamil Kornaus ², Szymon Wandor ³,
Julia Druciarek ³, Krzysztof Fitzner ¹ and Marek Wojnicki ^{1,*}

¹ Faculty of Non-Ferrous Metals, AGH University of Science and Technology, Mickiewiczza Ave. 30, 30-059 Krakow, Poland

² Faculty of Materials Science and Ceramics, AGH University of Science and Technology, Mickiewiczza Ave. 30, 30-059 Krakow, Poland

³ Technical Secondary School of Chemical and Environmental Protection No. 3, Krupnicza 44, 31-123 Krakow, Poland

* Correspondence: tomaszm@agh.edu.pl (T.M.); marekw@agh.edu.pl (M.W.); Tel.: +48-798-260-266 (T.M.); +48-601-183-889 (M.W.)

Abstract: This paper describes a single-stage synthesis process for activated carbon using cherry seeds. The influences of the carbonization temperature and the time were investigated. Using the BET method, the surface area of the obtained activated carbons was determined, as well as the pore distribution, while SEM images provided further insight into the structure of the surface. Next, the adsorption isotherm was derived. For the test, Pd(II) chloride complex ions were used. It was found that the obtained activated carbon were suitable for palladium(II) recovery from diluted aqueous solutions. Out of the tested parameters of carbon synthesis, the most optimal one was found to be 500 °C for 3 h. Additionally, it was confirmed that the increase in the adsorption temperature affects the increase in palladium load from 1.6 mg/g at 20 °C to 15.6 mg/g at 50 °C (for the best-performing sample). This fact may suggest that the process of adsorption is associated with chemical reactions.

Keywords: adsorption; activated carbon; palladium; recovery; recycling; sustainable technology



Citation: Michałek, T.; Wojtaszek, K.; Małecki, S.; Kornaus, K.; Wandor, S.; Druciarek, J.; Fitzner, K.; Wojnicki, M. Recovery of Pd(II) Ions from Aqueous Solutions Using Activated Carbon Obtained in a Single-Stage Synthesis from Cherry Seeds. *C* **2023**, *9*, 46. <https://doi.org/10.3390/c9020046>

Academic Editors: Jorge Bedia and Carolina Belver

Received: 29 March 2023

Revised: 21 April 2023

Accepted: 26 April 2023

Published: 28 April 2023



Copyright: © 2023 by the authors. Licensee MDPI, Basel, Switzerland. This article is an open access article distributed under the terms and conditions of the Creative Commons Attribution (CC BY) license (<https://creativecommons.org/licenses/by/4.0/>).

1. Introduction

Sorption processes are widely used in environmental and industrial applications for the removal of contaminants [1,2], as well as for the recovery of precious metals from aqueous solutions [3,4]. Activated carbons have been recognized as one of the most influential and versatile sorbents due to their high surface area, microporosity, and adsorption capacity toward various heavy metals [5,6]. Moreover, using activated carbon as sorbent may be eco-friendly as they can be derived from renewable resources and easily regenerated and reused.

Palladium (Pd) is a precious metal that recently has gained increasing attention due to its unique physical and chemical properties. Pd is widely used in various industrial applications, such as in catalysis [7,8], electronics [9], and jewelry [10], and it is also an essential component in automotive catalytic converters [11]. The industry of buying and reusing catalytic converters is very lucrative since catalytic converters hold up to 7 g of platinum (which is valued at around EUR 82), up to 7 g of palladium (which is valued at around EUR 411), and up to 2 g of rhodium (which is valued at around EUR 974). Globally, approximately 90 tons of platinum, 300 tons of palladium, and 30 tons of rhodium are utilized annually for the production of catalytic converters. However, Pd is considered a critical raw material due to its limited availability and high cost [12]. Therefore, developing efficient and cost-effective methods for recovering Pd from aqueous solutions has become

crucial in the sustainable management of this element [13]. A promising solution in this field is the use of activated carbon obtained from organic materials.

There is a growing interest in the use of bio-waste precursors in the synthesis of activated carbon. A particularly developed direction is the use of organic waste. Pyrolysis of this type of material allows one to obtain valuable sorption materials while reducing the need to store troublesome organic waste. Additional advantages of obtaining activated carbon from bio-waste precursors are their low price and high availability, which applies practically all over the world. This allows for logistically optimized sorbent production as the material can be synthesized locally, which affects its price and availability [14]. This is particularly important in countries with high environmental pollution, where processing organic waste not only reduces their amount in landfills, but also obtains a sorbent that allows one to adsorb toxins that have already penetrated groundwater and soil. It is, therefore, necessary to further develop technologies for the synthesis of activated carbon from organic waste, which could be implemented cheaply and quickly anywhere in the world. For this reason, single-stage processes that are as simple as possible will be favored.

In research works from around the world, examples of the synthesis of activated carbon from coconut shells [15–19], rice shells [20–22], banana peels [23], sugar cane [24–27], bamboo [28], apricot stones [29], grape seeds [29], cherry seeds [30,31], and many others can be found. Interestingly, the primary structure and naturally occurring chemical compounds in these materials affect the properties of the activated carbon obtained from them. Thanks to this, sorbents synthesized from different precursors may have different properties. Usually, the carbon obtained in the pyrolysis process requires another process in which its surface is activated, i.e., functional groups are attached to the surface carbon atoms, affecting the properties of the sorbent [32,33]. In this process, strong inorganic acids, alkalis, and oxidants are most often used [34–37]. Organic precursors contain chemical compounds that could allow one to activate carbon that is already in the pyrolysis process [38]. Thanks to this, it could be potentially possible to obtain activated carbon in this stage, which makes the process much simpler and less labor- and energy-intensive.

The sorption capacity of activated carbon can easily be tested with the use of noble metal ions as model systems and as a potential sorbent content [39]. Their high price is an economic basis for developing a technology for their recovery with the use of sensitized activated carbon. However, the sorption capacity of activated carbon can be successfully used for the sorption of heavy metals [40], dyes [41] and other toxins, especially at the low price of the obtained activated carbon.

This study focuses on the synthesis and sorption properties of activated carbon obtained from cherry seeds to recover Pd(II) from aqueous solutions. Cherry seeds are an abundant waste material generated from the food industry, and their use as a precursor for synthesizing activated carbon represents an eco-friendly and sustainable approach. The scale of cherry seed production is very large as the seed makes up about 7–15% of the fruit weight [42]. Although Turkey is the largest producer of cherries in the world (approximately 914,000 tons produced in 2020), Poland also produces significant amounts of this fruit (approximately 203,000 tons produced in 2020) [43]. This represents a large enough market to develop methods to utilize the seeds produced by the industry rather than simply treating them as waste.

The aim of this work is to investigate the sorption behavior of activated carbon derived from cherry seeds toward Pd(II) ions in aqueous solutions. The resulting carbon was characterized using scanning electron microscopy (SEM) and Brunauer–Emmett–Teller (BET) methods to determine their surface morphology and surface area, respectively. The effects of various parameters, such as solution temperature, the temperature of cherry seeds roasting, and initial Pd(II) concentration, on the sorption process will be evaluated. The sorption isotherms and kinetics of Pd(II) adsorption onto cherry-seed-derived activated carbon will also be determined. Additionally, the point of zero charges for the activated carbon obtained at different synthesis temperatures and times was determined to provide insights into their surface properties and potential applications.

Overall, the results of this study have the potential to contribute to the development of efficient and eco-friendly methods for the recovery of Pd from aqueous solutions while also promoting the usage of cherry seeds as a renewable resource for the synthesis of activated carbon.

2. Materials and Methods

Cherry seeds were first grounded and then dried for 5 h in 100 °C with a drying oven (VWR Collection, Lutterworth England). They were ground in a laboratory roller-ring mill (EKO-LAB, Brzesko, Poland) for 30 s. The ground seeds were roasted in a tube furnace (Czylok, Jastrzębie-Zdrój, Poland) in a nitrogen atmosphere (99.999%, Air Liquide, Kraków, Poland), with a flow rate of 20 L/h. The detailed parameters that were programmed into the furnace for individual samples are shown in Table 1.

Table 1. Programmed parameters in the furnace for our samples.

Sample Number	Synthesis Temperature [°C]	Synthesis Time [h]
1	400	1
2	400	2
3	400	3
4	500	3
5 ¹	500	3
6	600	3
7	700	3

¹ This sample was not dried before grinding.

Carbon obtained from roasting cherry seeds was already activated (which is proved in the following sections); hence, this single-stage synthesis was a success.

The obtained product was then analyzed to determine the exact influence of synthesis time, synthesis temperature, and drying of seeds before grinding on carbon functionality. The specific area of carbon was determined by BET analysis. Their adsorption capabilities were tested by placing them in solutions containing Pd(II) ions and then placing those solutions in a shaker (ELPIN, Lubawa, Poland) for four days between each measurement series to ensure that equilibrium concentration was reached. This shaker is equipped with a water bath thermostatic system.

Stock solutions containing Pd(II) chloride complex ions were prepared as described in our previous paper [44]. Next, a further dilution of stock solutions using 0.1 M HCl were made to obtain the desired concentrations. In this way, solutions with Pd(II) concentrations of 0.1, 0.25, 0.5, 1, and 2 mM were obtained. These solutions were used to carry out the adsorption tests of the activated carbon obtained from cherry seeds. In each measurement series, c.a. 0.334 g of carbon in 200 mL of solution was used. A spectrophotometer Jasco model V-770 (Tokyo, Japan) and Hellma GmbH (Müllheim, Germany) analytics quartz cuvettes (1 or 0.2 cm optical paths) were used to study the changes in Pd(II) concentrations over time.

In order to determine the point of zero charges (ZPC) for the activated carbon obtained with various synthesis parameters, as is described in Table 1, solutions with a pH of 2–12 were prepared. These solutions were based on 0.1 M NaNO₃, acidified with 0.1 M HClO₄, and alkalinized with 0.1 M NaOH. The pH of the solutions during ZPC determination was measured using a multifunctional ELMETRON CX-505 m (Zabrze, Poland). The device was calibrated before measurement using the three-point method and buffers with pH values of 1, 4, and 7 (POCH S.A., Gliwice, Poland).

BET measurements were carried out on a Micromeritics ASAP 2010 device. The samples were degassed at 200 degrees Celsius to a vacuum of 4 µmHg for 24 h. The measurement starts after obtaining a vacuum of 10 µmHg in the measuring cell, with the first measuring point at a pressure of 40–50 mmHg. The temperature of the measuring cell was set to 77.35 K, and each sample was measured five times with increasing relative pressure (the interval between measurements was 120 min).

The Fourier-transform infrared (FT-IR) spectra (Nicolet 380, Waltham, MA, USA) were determined. The FT-IR spectroscopy was performed using the transmission method. The sample was ground in an agate mortar with 0.2 g of KBr (Merck, Germany, Darmstadt). Since qualitative results will be sufficient for this analysis, we did not measure the specific masses of carbon for these measurements, while the specific mass of KBr served a purpose in achieving uniform pellets. Those pellets were prepared by using a punch with a 10 mm diameter and a hydraulic press that generated a pressure of up to 10 MPa.

Differential thermal analysis and differential scanning calorimetry, DSC-TGA, were used for the characterization process of the activated carbon synthesis with TA Instruments SDT Q.600 (TA Instrument, New Castle, DE, USA). Thermal analyses of the cherry pit materials were conducted in an air/Ar atmosphere with the flow of the gas equal to 100 mL/min unless otherwise stated.

3. Results

3.1. Effect of Synthesis Parameters on the Surface Area

The effect of the activated carbon's synthesis parameters was investigated to determine their impact on the resulting activated carbon properties. This study analyzed the influence of synthesis temperature and the drying of the seeds before synthesis on specific surface areas of obtained activated carbon. The results of the BET analysis are shown in Figure 1.

Figure 1a shows that increasing the synthesis temperature from 500 °C to 600 °C results in an increase in the specific surface area of the activated carbon. During roasting, the volatile organic compounds within the cherry seeds are removed, leaving behind a carbonaceous residue. As the roasting temperature increases, the carbonaceous residue is subjected to thermal decomposition, which results in the formation of new pores and the expansion of existing ones. This, in turn, increases the surface area of the activated carbon. However, too high a synthesis temperature can destroy the carbon structure, resulting in a decrease in surface area and pore volume, which explains the significant decrease found in the surface area of carbon roasted at 700 °C. The BET analysis of carbon obtained by the synthesis at 400 °C resulted in an error. At low synthesis temperatures, the carbon structure may not be fully activated and the resulting activated carbon may have fewer and smaller pores than the activated carbon prepared at higher temperatures. This can lead to a lack of uniformity in pore size and shape, resulting in errors in the BET analysis. The BET method relies on a homogeneous surface for the accurate measurement of specific surface areas, so a lack of uniformity in the pore structure of the activated carbon can result in an inaccurate or unreliable BET analysis. Therefore, optimizing the synthesis parameters during the preparation of activated carbon is important to ensure that the resulting material has a uniform pore structure and is suitable for analysis by the BET method. Figure 2b shows that drying the seeds before roasting makes virtually no difference in the resulting surface area compared to seeds that were not dried.

In order to better characterize the structure of the obtained carbons, a longer analysis was conducted for Sample no. 5. Figure 2c shows detailed N₂ adsorption and desorption isotherms for this sample, which provides further insight into the porous structure of our AC. It is important to note that the desorption curve should have a decreasing course with increasing pressure, while in our case there is an area where this trend is reversed. This is a result of the evaporation of nitrogen from the Dewar during the measurement since this measurement lasted for over 30 h. Figure 1d shows the pore distribution in our carbon sample. As can be seen, the nanopores are the leading contributors to the overall volume of pores in the AC. Due to this fact, our AC may be more suited for adsorption of gases since nanopores can be too small to efficiently adsorb large complex molecules/ions. In addition, the wettability of its surface for solvent is also difficult to use.

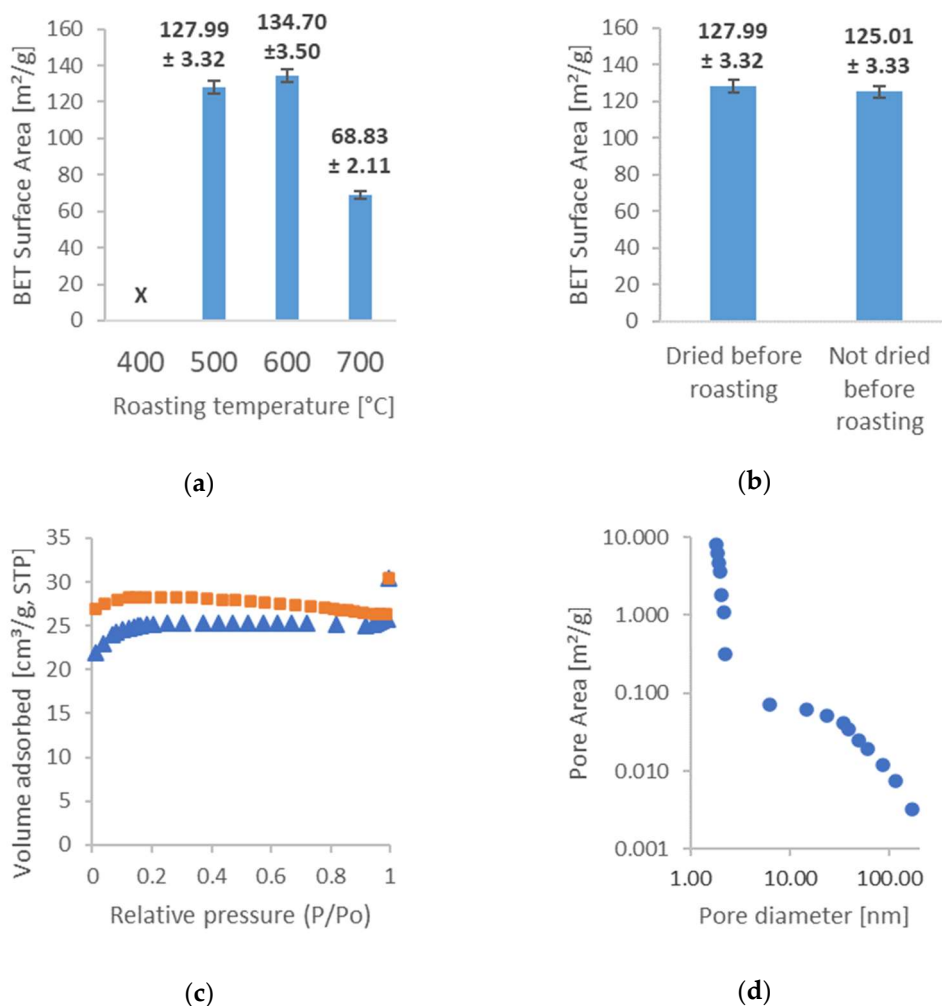


Figure 1. Results of the BET analysis: (a) influence of synthesis temperature on surface areas; (b) influence of drying the seeds on surface areas before synthesis; (c) an example of adsorption and desorption isotherms (Sample no. 4); and (d) an example of the pore distribution obtained from BJH adsorption analysis (Sample no. 4).

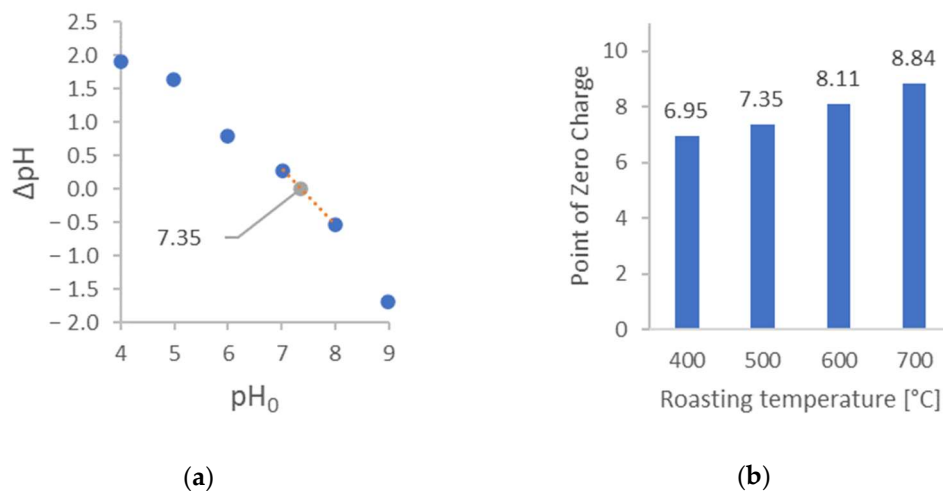


Figure 2. Cont.

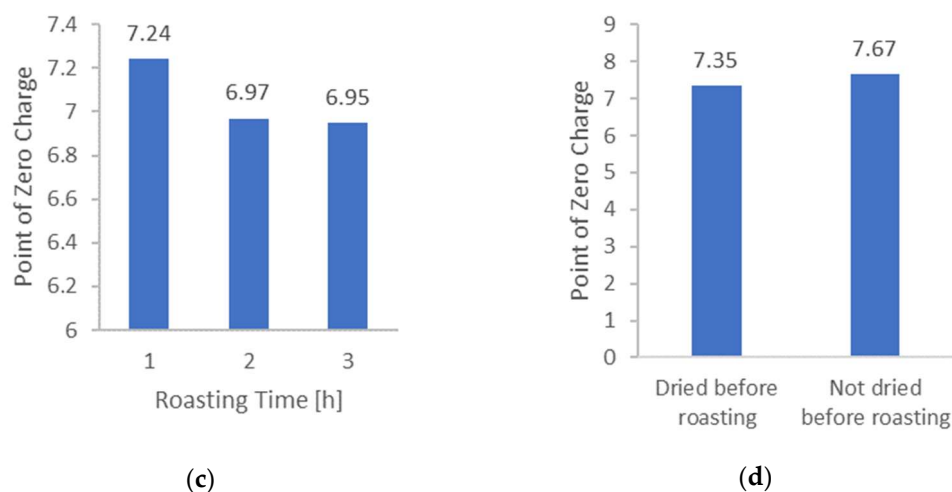


Figure 2. Effects of synthesis parameters on the PZC of the obtained activated carbon: (a) example showing how to determine PZC (Sample no. 4); (b) influence of synthesis temperature; (c) influence of synthesis time; and (d) influence of drying the seeds before synthesis.

3.2. Effect of Synthesis Parameters on the Point of Zero Charge

The point of zero charge (PZC) of the activated carbon is an important characteristic that determines the surface charge behavior of the material under various environmental conditions. The PZC of activated carbon is defined as the pH at which the material's surface carries no net electrical charge. Below the PZC, the surface of the material is positively charged, while above the PZC, the surface is negatively charged. At the PZC, the material's surface is neutral and has no net electric charge. This is an important parameter that affects the ion adsorption capabilities of activated carbon. In this study, we investigated the effect of the synthesis parameters on the PZC of the activated carbon prepared from cherry seeds. These results are gathered in Figure 2.

Figure 2a presents an example curve that was used to determine the PZC. Next, Figure 2b presents the influence of the synthesis temperature of AC on the PZC. As can be seen, higher temperature results in a higher value of PZC. Functional groups with lower stability dissociate more quickly, undergoing thermal degradation more easily. This may explain the shift of ZPC toward higher pH values. Figure 2c presents the influence of the synthesis time of AC on the ZPC. As can be seen, the increase in synthesis time results in a lower value of ZPC. However, the difference between synthesis in 2 and 3 h is negligible.

It should be noted that the first step of AC synthesis is the distillation of volatile organic compounds. Most likely, during the first hour, not all the compounds evaporated. Therefore, the ZPC of this coal is very high. It is also worth recalling the results of BET measurements, which suggested that the complete carbonization process had not occurred. Figure 2d shows the results related to the pre-treatment of the sample before AC synthesis. During drying, the aroma was perceptible. This proves the release of volatile organic compounds. Thus, pre-dried material undergoes the carbonization process differently than non-dried ones. This is an exciting observation that has not been previously reported in the literature.

The optimal synthesis conditions for preparing activated carbon with a low PZC were a temperature of 400 °C and a synthesis time of 3 h. Under these conditions, the activated carbon exhibited a PZC of 6.95 (closest to 7), which is favored for it not being a charged $[\text{PdCl}_2(\text{H}_2\text{O})_2]$ complex adsorption.

3.3. DSC-TGA Analysis of Cherry Pits

The thermal analysis of cherry pits enables the determination of several key parameters. Analysis was conducted in two different atmospheres: in argon and in air. Samples

analyzed in argon were later subjected to tests in air atmosphere, and three tests of this type were conducted. The results of these tests are shown in Figure 3.

The tests in an argon atmosphere correspond to the conditions required for synthesizing activated carbon from cherry seeds. The first observed exothermic peak in Figure 3a at the beginning of analysis was commonly observed during the pyrolysis process of the biomass, and a slow decline of the sample mass was caused mainly due to the evaporation of moisture [45]. The intense decline of sample mass occurring after the temperature reached about 250 °C is a result of the gradual decomposition of the organic compounds contained in the plant tissues, while the slight change in the speed of this decline after reaching about 350 °C is related to char degradation. Analysis of the air atmosphere allows us to determine the total ash content in cherry seeds. It also makes it possible to check whether the observed peaks are endothermic and whether they may be related to the evaporation of volatile fractions. The results obtained are shown in Figure 3b. Finally, the ignition temperature was investigated (see Figure 3c). As can be seen, the activated carbon ignited at 492 °C. This is valuable information from the point of view of coal exploitation [46].

These results demonstrate the importance of analyzing materials under different environmental conditions to fully understand their properties and behavior. TG and DTG curves only reflect mass changes with temperature, and the changing trends of heat in the whole process cannot be understood through them [47]. Additional information that can be obtained from DSC-TGA analysis is the potential energy consumption of the process when producing active carbons from such a precursor. Of course, we are talking here about the energy necessary for the changes inside the precursor and not taking into account heat losses, etc.

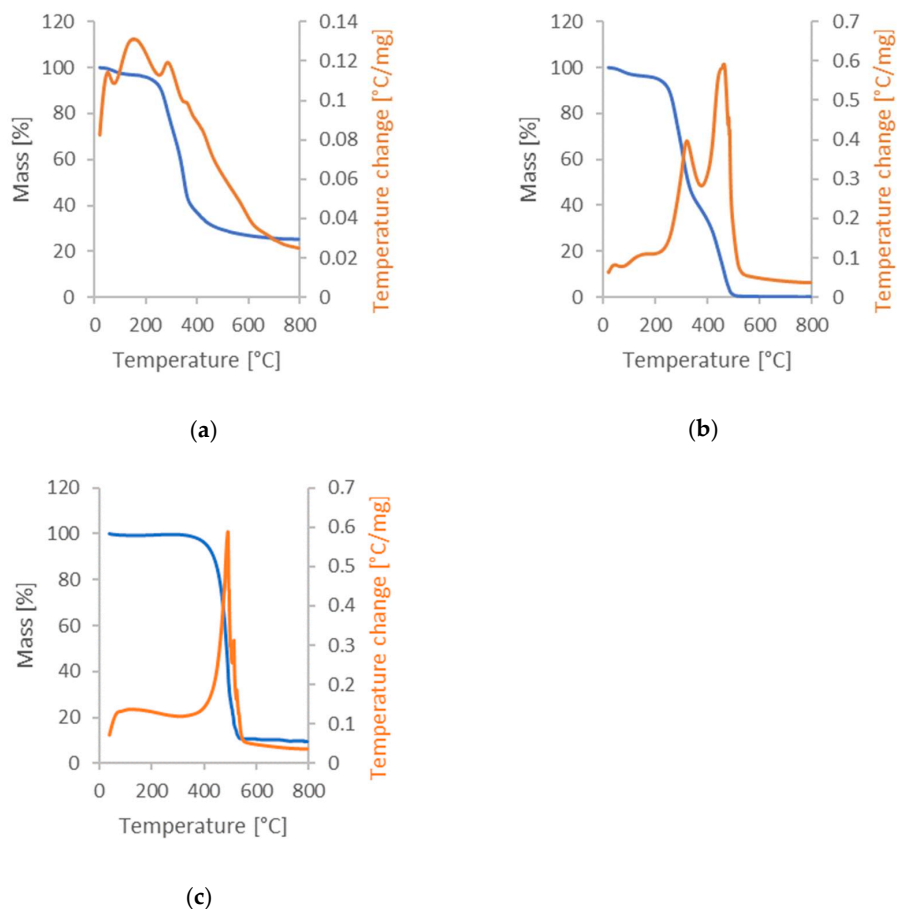


Figure 3. Results of the DSC-TGA analysis: (a) sample in argon atmosphere; (b) sample in air atmosphere; and (c) sample previously analyzed in argon, later subjected to test in air atmosphere.

3.4. FT-IR Analysis of Activated Carbon

The FT-IR analyses were performed for all the obtained AC samples. This analysis may provide evidence of the presence of functional groups in a carbon, and comparing results for the individual samples gives information about which one has more of them in those groups (sample with a higher number of peaks will naturally have more functional groups). For this purpose, the AC samples were triturated with KBr, which has a 100% IR transmittance. The crystal was then pressed out and analyzed. The obtained results are shown in Figure 4.

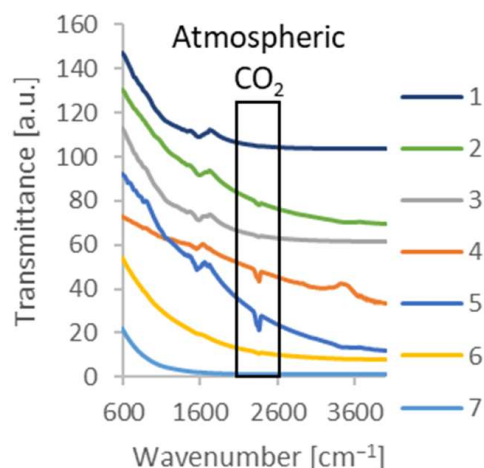


Figure 4. FT-IR spectra of the synthesized carbon. Numbers in the legend correspond to the numbers of the samples in Table 1.

Figure 4 shows that temperature and synthesis time significantly affected the functional groups of the activated carbon. The analysis revealed that the carbon obtained at higher temperatures generally showed smaller peaks in the FT-IR spectra. This suggests that the higher temperature used during synthesis led to the destruction of the functional groups responsible for the characteristic peaks in the FT-IR spectra.

The decrease in the number of functional groups in the activated carbon samples synthesized at higher temperatures can be attributed to their breakdown in the precursor during the process. As the temperature increases, the chemical bonds become weaker and are more prone to breaking. This results in the removal of functional groups. On the one hand, the presence of functional groups on the surface improves the wettability of activated carbon by water [48]; on the other hand, the deprotonation of functional groups causes the formation of a surface charge, which can block the adsorption of electrically non-neutral particles [49].

In general, the FT-IR analysis provided valuable insights into the changes in the chemical structure of activated carbon due to synthesis. The results suggest that the synthesis conditions may significantly influence the properties of the activated carbon, and understanding these changes is crucial for optimizing the production of activated carbon with desired properties.

3.5. Adsorption Properties of Carbon

The adsorption properties of the activated carbon were evaluated by measuring the Pd(II) concentration in the solution before and after contact with the activated carbon. The Pd(II) concentration was determined with a spectrophotometer by measuring the absorbance of the Pd(II) chlorine complex at a wavelength of 278 nm. It has already been well documented in the literature that the molar absorption coefficient of Pd(II) ions at a wavelength of 278 nm is equal to $5980 \text{ dm}^3 \text{ cm}^{-1} \text{ mol}^{-1}$ [50], and this standard fits well with our experimental data.

In order to estimate the required time to attain equilibrium in the system, the kinetics of adsorption for one of our samples was investigated. The result is shown in Figure 5.

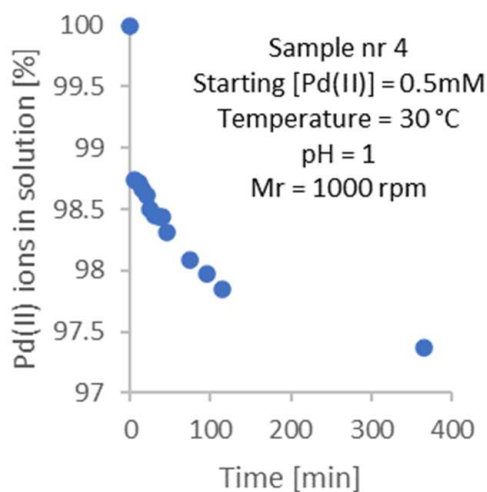


Figure 5. An example of the kinetic curve for the adsorption process of Pd(II) ions for Sample no. 4 (see Table 1).

As can be seen, the process is fast. Significant changes occur in the first 100 min. Extending the experiment to 400 min causes further changes of no more than 0.3%. Therefore, for the purposes of future work, it was assumed that equilibrium is reached after a minimum of 96 h; this was assumed to ensure that the equilibrium was surely reached.

The Freundlich isotherms were constructed by applying a logarithmic version of the Freundlich Equation (1) to our data, which allowed us to calculate the adsorption capacity (X/m). This equation looks as follows [51]:

$$\log \frac{X}{m} = \log K + \frac{1}{n} \log C_{eq} \quad (1)$$

where X is total mass of the Pd adsorbed (mg); m is the weight of the adsorbent, in this case activated carbon (g); and K and n , at a given temperature, remain constant for a particular adsorbate and adsorbent.

X/m can be calculated using the following Equation (2). It looks as follows [51]:

$$\frac{X}{m} = \frac{(C_0 - C_{eq}) \times V}{m} \quad (2)$$

where C_0 and C_{eq} (mol/L) are the starting concentration and final concentration of Pd, respectively, and the volume of the mixture (L) is represented by V .

The constants K and n were determined by plotting the logarithm of the amount of Pd(II) adsorbed per unit weight of the activated carbon ($\log(X/m)$) against the logarithm of the Pd(II) equilibrium concentration in solution ($\log(C)$). Another way of presenting the adsorption capacity of an adsorbent is to correlate it to the initial concentration of the pollutant [52] or to its equilibrium concentration [53]. That is why we constructed graphs showing the mass of the Pd(II) adsorbed per mass of carbon (X/m) for their respected equilibrium concentrations. Results for sample nos. 3, 4, and 6 (see Table 1) are shown in Figures 6 and 7, and the obtained values of constants K and n are presented in Table 2.

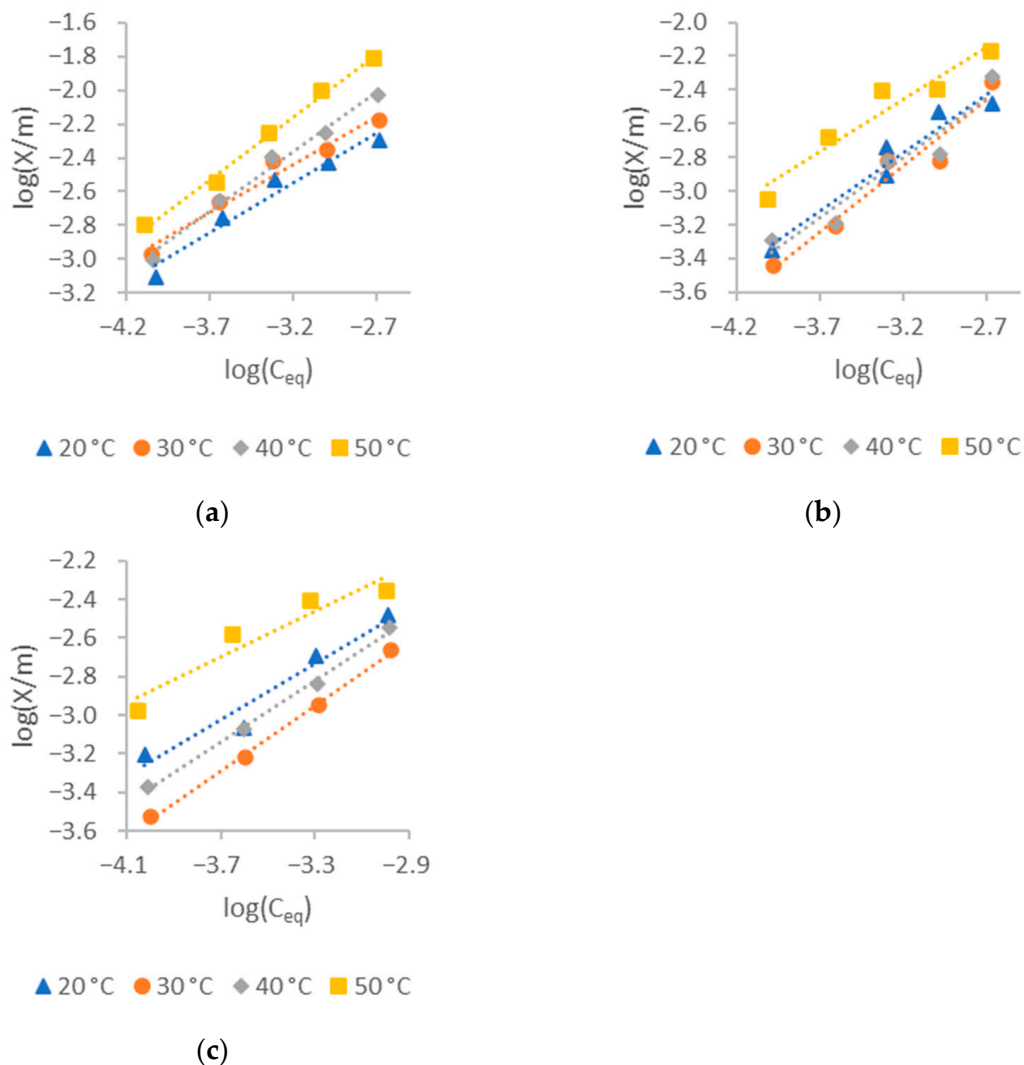


Figure 6. Freundlich isotherms of the synthesized carbons: (a) synthesis temperature of carbon = 400 °C (Sample no. 3); (b) synthesis temperature of carbon = 500 °C (Sample no. 4); and (c) synthesis temperature of carbon = 600 °C (Sample no. 6).

Table 2. The constants *K* and *n* obtained from Freundlich isotherms.

Sample Number	Mixture Temperature [°C]	<i>K</i> [(mg/g)(L/mol) ^{<i>n</i>}]	<i>n</i>
3	20	0.22	1.69
	30	0.24	1.76
	40	0.80	1.41
	50	1.73	1.34
4	20	0.28	1.44
	30	0.46	1.27
	40	0.29	1.41
	50	0.31	1.64
6	20	0.49	1.36
	30	0.72	1.18
	40	0.67	1.25
	50	0.31	1.69

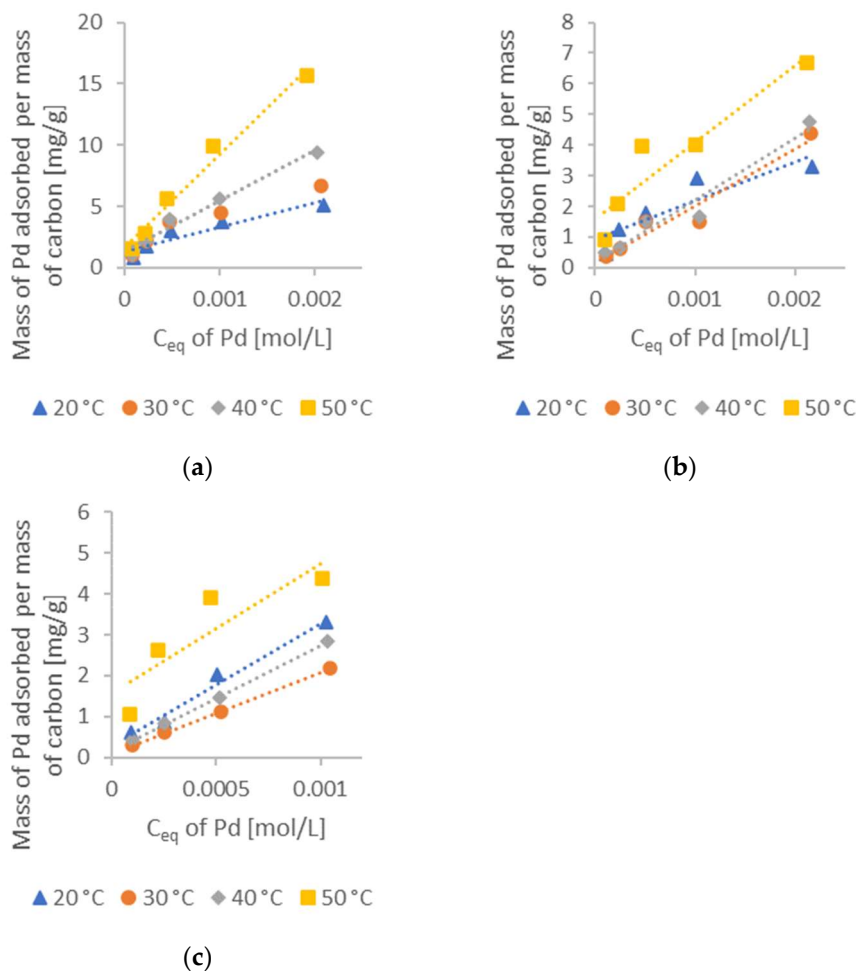


Figure 7. Mass of the Pd(II) adsorbed per mass of synthesized carbons: (a) synthesis temperature of carbon = 400 °C (Sample no. 3); (b) synthesis temperature of carbon = 500 °C (Sample no. 4); and (c) synthesis temperature of carbon = 600 °C (Sample no. 6).

Figures 6c and 7c consist of only four different equilibrium concentrations (while the other graphs consist of five) because they lost their tightness, and the sample was contaminated with coolant from the thermostat.

Figures 6 and 7 show that the activated carbon obtained from the cherry seeds exhibited excellent sorption properties for the Pd(II) from aqueous solutions, while Table 2 shows the obtained values of constants K and n . The adsorption capacity of the activated carbon decreased with increases in the synthesis temperature. The activated carbon roasted at 400 °C for 3 h exhibited the highest adsorption capacity, and had the highest mass of Pd(II) adsorbed per mass of carbon (15.6 mg/g), which is shown in Figure 7a. Increasing the temperature of synthesis from 400 to 500 °C (Figure 7b) resulted in a maximum adsorption capacity decrease to 7.1 mg/g, which is less than half of the previously achieved result. Figure 7c represents the result of a further increase in synthesis temperature to 600 °C. However, due to the previously mentioned issue with the mixer, we cannot compare this graph with values mentioned in Figure 7b,c, since they correspond to the initial concentration of 2 mM. We can, however, compare the results for the initial concentration of 1 mM. For the sample roasted at 600 °C, the maximum adsorption capacity was 4.4 mg/g, while this capacity for the samples synthesized at 400 and 500 °C was 9.9 and 4 mg/g, respectively.

It was observed that an increase in adsorption temperature favored an increase in adsorption capacity. This is the opposite effect to the typical phenomena of physical adsorption from the gas phase. However, it should be borne in mind that Pd(II) adsorption is carried out from aqueous solutions. In the aqueous phase, Pd(II) has several different

equilibrium forms. In Pd(II) the $\text{Cl}^- - \text{H}_2\text{O}$ system at $\text{pH} = 1$ is the most dominant form and should be $[\text{PdCl}_2(\text{H}_2\text{O})_2]$ at approximately 55.87%, with $[\text{PdCl}_3(\text{H}_2\text{O})]^-$ being the second most dominant at 39.03% [54]. These equilibria also depend on temperature. An increase in temperature shifts the equilibrium of Pd(II) compounds in such a way that the preferentially adsorbed form has a higher activity (concentration). Therefore, the adsorption capacity increases with increasing temperature. For this reason, a thermodynamic analysis of the adsorption process should be carried out with great care. Positive Gibbs free energy is often observed for adsorption processes, especially for adsorptions that are conducted at the condensed phase. There is a fundamental error here in assuming that only one process depends on temperature.

3.6. SEM Images and EDS Analysis

Scanning electron microscopy (SEM) images were taken to investigate the surface morphology and pore structure of the activated carbons synthesized from cherry seeds, as well as to observe how the Pd was distributed on its surface after the adsorption process. The SEM images were taken for the activated carbon, which performed best in the adsorption experiments (Sample no. 3) when using the JEOL-6000 Plus instrument (Tokyo, Japan). Energy-dispersive X-ray spectroscopy (EDS) analysis was conducted as well to provide some insight into the chemical composition of our samples. The results are shown in Figures 8 and 9, as well as in Tables 3 and 4.

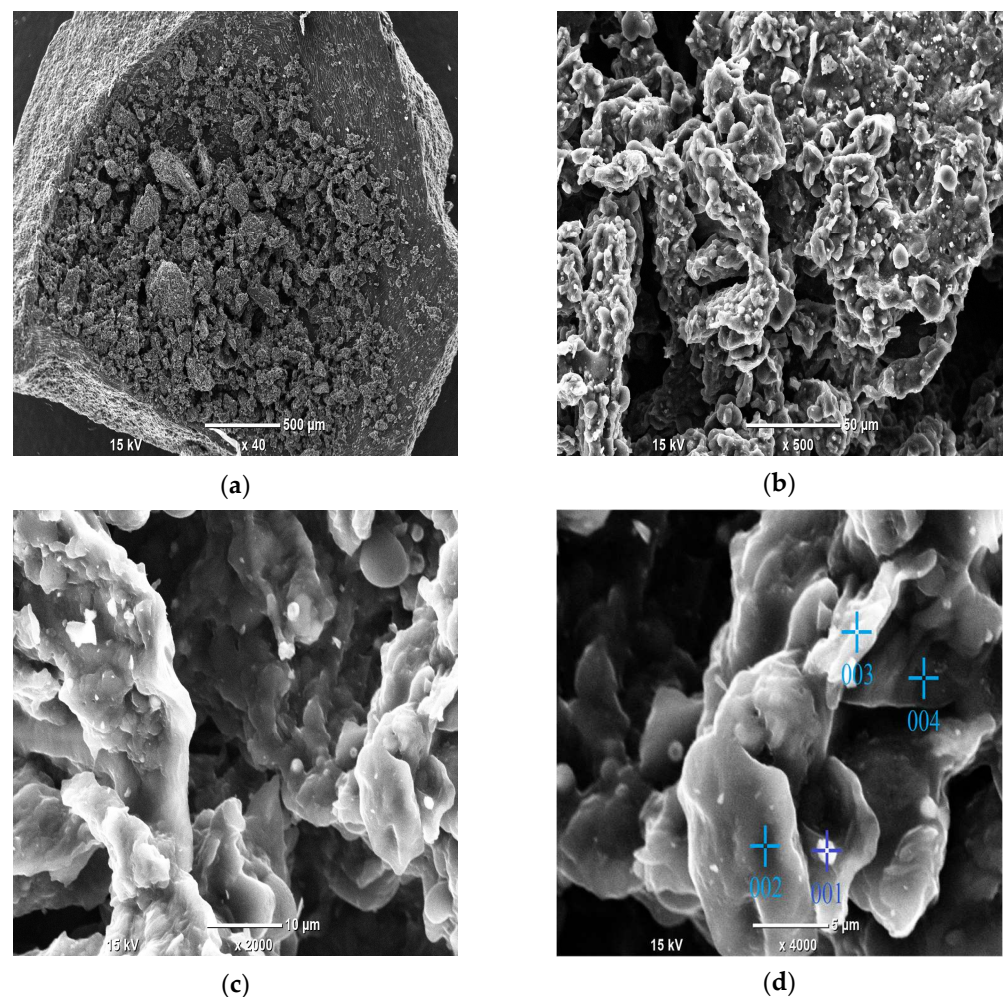


Figure 8. SEM images of the activated carbon (Sample no. 3) before the adsorption process at different magnifications: (a) 40× magnification; (b) 500× magnification; (c) 2000× magnification; and (d) 4000× magnification (with marked points subjected to EDS analysis).

Table 3. Results of EDS analysis for the AC before the adsorption process (Sample no. 3). Point numbers correspond to the point numbers in Figure 8d.

Point Number	Mass %							
	C	N	O	Mg	Si	P	K	Ca
001	70.48	4.31	22.42	0.62	0.02	0.87	0.92	0.36
002	90.09	ND	9.27	0.02	0.33	0.06	0.18	0.04
003	81.33	2.41	14.67	0.20	0.36	0.45	0.32	0.26
004	85.34	ND	12.76	0.30	0.39	0.50	0.54	0.16

Figure 8 shows the SEM images of the activated carbon obtained from cherry seeds at different magnifications. At low magnification (Figure 8a, 40 \times), the surface of the activated carbon appears to be quite smooth at the outer parts and porous in the center. At medium magnification (Figure 8b, 500 \times), the presence of micropores can be observed, which are formed due to the removal of organic volatile matter during the activation process. The micropores are well distributed throughout the surface of the activated carbon, providing a sufficient surface area for adsorption. High magnifications (Figure 8c,d, i.e., 2000 \times and 4000 \times , respectively) provide further insight into the structure of our AC. The surface was highly porous, and some white points can be observed, which indicates that something was already adsorbed onto our carbon. The EDS analysis (Table 3) shows that the white points are parts of the material containing nitrogen, among other elements such as Mg, P, K and Ca, all of which are essential for all living things, including plants. Cherry seeds naturally have to contain these elements; therefore, it is not surprising that our AC also contains them.

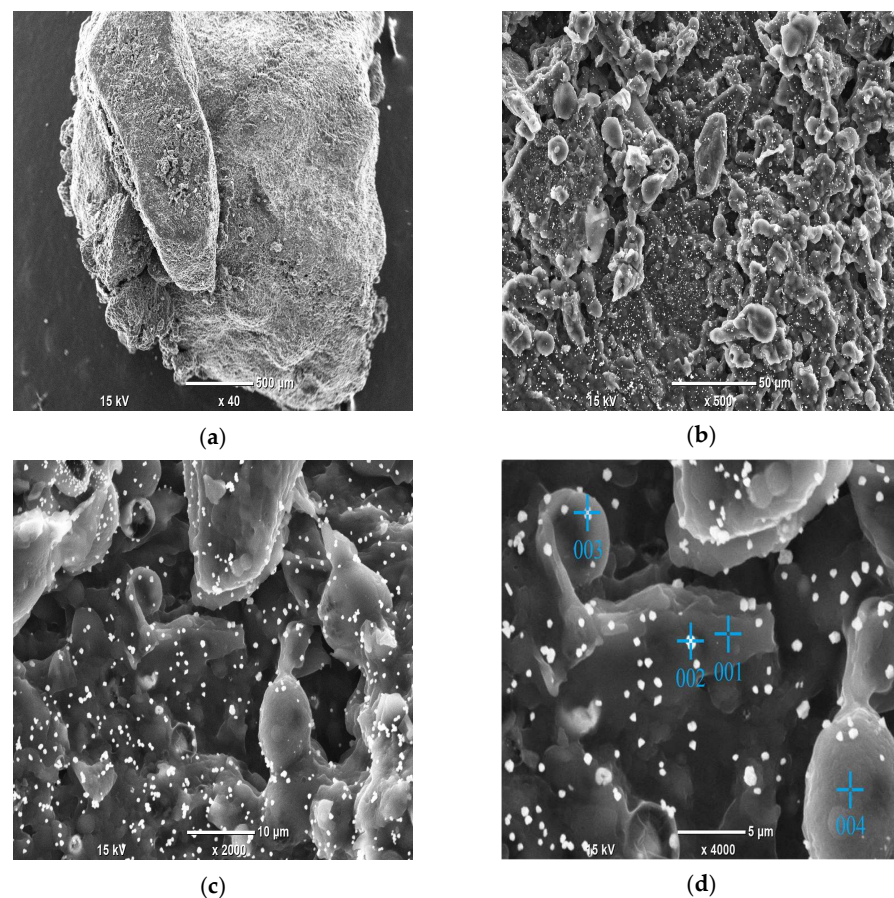


Figure 9. SEM images of the activated carbon (Sample no. 3) after the Pd (II) adsorption process at different magnifications: (a) 40 \times magnification; (b) 500 \times magnification; (c) 2000 \times magnification; and (d) 4000 \times magnification (with the marked points subjected to EDS analysis).

Table 4. Results of the EDS analysis for AC after the Pd(II) adsorption process (Sample no. 3). Point numbers correspond to the point numbers in Figure 9d.

Point Number	Mass %						
	C	N	O	Si	P	Cl	Pd
001	69.58	8.29	20.83	0.29	0.11	0.84	0.05
002	56.73	ND	26.58	0.52	0.18	0.62	15.38
003	57.98	11.40	14.94	0.13	0.89	4.66	9.99
004	75.89	5.52	8.22	1.25	1.28	7.24	0.61

Figure 9 shows the SEM images of our activated carbon after the Pd(II) adsorption process. At low magnification (Figure 9a, 40 \times), the surface does not appear to be very porous; in fact, it looks quite smooth. At medium magnification (Figure 9b, 500 \times), the porous structure can be observed, as well as multiple small white points. High magnifications (Figure 9c,d, 2000 \times and 4000 \times) reveal that those white points are quite evenly distributed in the observed fragment of the carbon surface. Considering the fact that these images were taken after the process of Pd(II) adsorption, the white points are probably Pd particles. This was confirmed by EDS analysis (Table 4), which revealed high Pd content in those areas, while also showing that, outside of them, the Pd content is negligible.

The SEM images and EDS analysis provided further evidence that AC made from cherry seeds is suited for the adsorption of Pd.

4. Discussion

The synthesis and sorption properties of activated carbon obtained from cherry seeds in the process of Pd(II) recovery from aqueous solutions were investigated in this study. In this section, we will discuss the study's key findings and their implications, as well as compare them with previous research in the field.

The results of this study demonstrate that activated carbon from cherry seeds have a high adsorption capacity for Pd(II) ions from aqueous solutions. The activated carbon was characterized by DSC-TGA, FT-IR, and BET analysis, which confirmed their surface area and surface functionality to not be that high, especially for carbon synthesized in elevated temperatures. However, their sorption capacity was found to be quite acceptable. A comparison of our AC with some commercially available AC is shown in Table 5.

Table 5. Comparison of AC for Pd(II) adsorption.

Reference	Maximum Adsorption Capacity [mg/g]	pH	Adsorbent Dose [g/L]	Initial Pd(II) Concentration [M]	Temperature [$^{\circ}$ C]
This study (Sample no. 3)	15.6	1	1.67	0.002	50
This study (Sample no. 4)	6.69	1	1.67	0.002	50
This study (Sample no. 5)	4.37	1	1.67	0.001	50
[55]	27	1	5–7.5	0.0018	25
[56]	35.7	2	6	0.0009	45
[57]	51.6	1	0.61	0.1	20
[57]	41.4	1	0.7	0.1	20

As can be seen in Table 3, the Pd(II) adsorption capacity of our AC (synthesized in 400 $^{\circ}$ C, Sample no. 3) was not significantly smaller when compared to some commercially available AC (which were found in the literature). Since low-cost adsorbents made from agricultural, industrial, and natural materials tend to have inferior adsorption properties compared to adsorbents made from high-end materials in well-optimized conditions, our carbon made from cherry seeds have huge potential. Moreover, the utilization of cherry seeds, which are a byproduct of the food industry, for the synthesis of activated carbon can provide a sustainable and eco-friendly approach to the recovery of Pd(II) ions from aqueous

solutions. Our AC synthesized in 500 °C (Sample no. 4) and 600 °C (Sample no. 5) were characterized by very poor adsorption capacity, which is further highlighted by comparison to commercially available AC. As we stated in previous subsections, optimizing synthesis parameters is crucial to obtain the most efficient AC possible, and this also means that it is likely possible to obtain carbon from cherry seeds, which will have higher adsorption capacities than our best performing sample (no. 3).

5. Conclusions

Based on the presented results, the following conclusions can be drawn:

- The temperature and time of the synthesis have an immense effect on the properties of the resulting carbon. Increasing the synthesis temperature from 500 °C to 600 °C resulted in drastically degrading the carbon specific area. Synthesis parameters also significantly affected the PZC of the obtained carbon—the PZC decreased with longer synthesis time and increased with higher synthesis temperatures. Elevated synthesis temperatures also negatively affected the presence of the functional groups in the obtained carbon, which was shown by the FT-IR tests;
- Adsorption tests showed a near-linear correlation between the adsorption capacity of the carbon and equilibrium Pd(II) concentrations. The highest value for adsorption capacity we obtained was 15.6 mg/g, which was for carbon synthesized at 400 °C for 3 h. Carbon synthesized in elevated temperatures showed worse adsorption properties, thus corresponding with other tests we conducted (such as FT-IR showing less functional groups for those carbons). It is very likely that further optimization of synthesis parameters will result in AC that will outperform our sample synthesized at 400 °C;
- Pd(II) adsorption from aqueous solutions was carried out, where several different equilibrium forms were present. In the Pd(II)–Cl[−]–H₂O system at pH = 1, the most dominant form is [PdCl₂(H₂O)₂] at approximately 55.87%. Since the activated carbon surface is negatively charged at pH = 1 (as concluded by determination of the PZC), it is suggested that this complex is preferably adsorbed as all other complexes are negatively charged and thus will be repelled from AC. The only exception would be a [PdCl(H₂O)₃]⁺ complex, which will be attracted to negatively charged AC; however, it has a miniscule share of about 3.37% [50].

Author Contributions: Conceptualization, M.W.; methodology, M.W.; validation, M.W. and K.F.; formal analysis, T.M. and K.W.; investigation, S.W., J.D., S.M., K.K. and K.W.; data curation, T.M.; writing—original draft preparation, T.M.; writing—review and editing, T.M.; visualization, T.M.; supervision, M.W.; project administration, M.W. and K.W. All authors have read and agreed to the published version of the manuscript.

Funding: This research was financed from the funds of the Faculty of Non-Ferrous Metals of AGH in Krakow, as well as supported by the National Science Center of Poland under grand number 2016/23/D/ST8/00668 Sontata 12.

Data Availability Statement: The datasets used and/or analyzed during the current study are available from T. Michałek (tomaszm@agh.edu.pl) upon reasonable request.

Conflicts of Interest: The authors declare no conflict of interest.

References

1. Yin, C.Y.; Aroua, M.K.; Daud, W.M.A.W. Review of modifications of activated carbon for enhancing contaminant uptakes from aqueous solutions. *Sep. Purif. Technol.* **2007**, *52*, 403–415. [[CrossRef](#)]
2. Li, L.; Quinlivan, P.A.; Knappe, D.R. Effects of activated carbon surface chemistry and pore structure on the adsorption of organic contaminants from aqueous solution. *Carbon* **2002**, *40*, 2085–2100. [[CrossRef](#)]
3. Mpinga, C.N.; Bradshaw, S.M.; Akdogan, G.; Snyders, C.A.; Eksteen, J.J. The extraction of Pt, Pd and Au from an alkaline cyanide simulated heap leachate by granular activated carbon. *Miner. Eng.* **2014**, *55*, 11–17. [[CrossRef](#)]

4. Chand, R.; Watari, T.; Inoue, K.; Kawakita, H.; Luitel, H.N.; Parajuli, D.; Torikai, T.; Yada, M. Selective adsorption of precious metals from hydrochloric acid solutions using porous carbon prepared from barley straw and rice husk. *Miner. Eng.* **2009**, *22*, 1277–1282. [[CrossRef](#)]
5. Lo, S.F.; Wang, S.Y.; Tsai, M.J.; Lin, L.D. Adsorption capacity and removal efficiency of heavy metal ions by Moso and Ma bamboo activated carbons. *Chem. Eng. Res. Des.* **2012**, *90*, 1397–1406. [[CrossRef](#)]
6. Guo, M.; Qiu, G.; Song, W. Poultry litter-based activated carbon for removing heavy metal ions in water. *Waste Manag.* **2010**, *30*, 308–315. [[CrossRef](#)]
7. Guo, L.; Gao, H.; Guan, Q.; Hu, H.; Deng, J.; Liu, J.; Liu, F.; Wu, Q. Substituent effects of the backbone in α -diimine palladium catalysts on homo- and copolymerization of ethylene with methyl acrylate. *Organometallics* **2012**, *31*, 6054–6062. [[CrossRef](#)]
8. Paul, S.; Clark, J.H. Structure-activity relationship between some novel silica supported palladium catalysts: A study of the Suzuki reaction. *J. Mol. Catal. A Chem.* **2004**, *215*, 107–111. [[CrossRef](#)]
9. Hughes, A.E.; Haque, N.; Northey, S.A.; Giddey, S. Platinum group metals: A review of resources, production and usage with a focus on catalysts. *Resources* **2021**, *10*, 93. [[CrossRef](#)]
10. Corti, C.W. The 23rd Santa Fe symposium on jewelry manufacturing technology. *Platin. Met. Rev.* **2009**, *53*, 198–202. [[CrossRef](#)]
11. Xu, B.; Chen, Y.; Zhou, Y.; Zhang, B.; Liu, G.; Li, Q.; Yang, Y.; Jiang, T. A Review of Recovery of Palladium from the Spent Automobile Catalysts. *Metals* **2022**, *12*, 533. [[CrossRef](#)]
12. Massari, S.; Ruberti, M. Rare earth elements as critical raw materials: Focus on international markets and future strategies. *Resour. Policy* **2013**, *38*, 36–43. [[CrossRef](#)]
13. Birinci, E.; Gülfe, M.; Aydın, A.O. Separation and recovery of palladium(II) from base metal ions by melamine-formaldehyde-thiourea (MFT) chelating resin. *Hydrometallurgy* **2009**, *95*, 15–21. [[CrossRef](#)]
14. Sandarenu, P.C.; Samaraweera, G.C. Export market of coconut shell charcoal and coconut shell activated carbon in Sri Lanka: Drivers and bottlenecks. In Proceedings of the Greener Agriculture and Environment through Convergence of Technologies, University of Ruhuna, Matara, Sri Lanka, 19 January 2017.
15. Sujiono, E.H.; Zabrian, D.; Zharvan, V.; Humairah, N.A. Fabrication and characterization of coconut shell activated carbon using variation chemical activation for wastewater treatment application. *Results Chem.* **2022**, *4*, 100291. [[CrossRef](#)]
16. Lutfi, M.; Hanafi, Susilo, B.; Prasetyo, J.; Sandra; Prajogo, U. Characteristics of activated carbon from coconut shell (*Cocos nucifera*) through chemical activation process. *IOP Conf. Ser. Earth Environ. Sci.* **2021**, *733*, 012134. [[CrossRef](#)]
17. Keppetipola, N.M.; Dissanayake, M.; Dissanayake, P.; Karunarathne, B.; Dourges, M.A.; Talaga, D.; Servant, L.; Olivier, C.; Toupance, T.; Uchida, S.; et al. Graphite-type activated carbon from coconut shell: A natural source for eco-friendly non-volatile storage devices. *RSC Adv.* **2021**, *11*, 2854–2865. [[CrossRef](#)] [[PubMed](#)]
18. Lima, S.B.; Borges, S.M.S.; Do Carmo Rangel, M.; Marchetti, S.G. Effect of iron content on the catalytic properties of activated carbon-supported magnetite derived from biomass. *J. Braz. Chem. Soc.* **2013**, *24*, 344–354. [[CrossRef](#)]
19. Kwasi Opoku, B.; Isaac, A.; Akrofi Micheal, A.; Kwesi Bentum, J.; Paul Muyoma, W. Characterization of Chemically Activated Carbons Produced from Coconut and Palm Kernel Shells Using SEM and FTIR Analyses. *Am. J. Appl. Chem.* **2021**, *9*, 90. [[CrossRef](#)]
20. Le Van, K.; Luong Thi, T.T. Activated carbon derived from rice husk by NaOH activation and its application in supercapacitor. *Prog. Nat. Sci.* **2014**, *24*, 191–198. [[CrossRef](#)]
21. Ahiduzzaman, M.; Sadrul Islam, A.K.M. Preparation of porous bio-char and activated carbon from rice husk by leaching ash and chemical activation. *Springerplus* **2016**, *5*, 1248. [[CrossRef](#)]
22. Alam, M.M.; Hossain, M.A.; Hossain, M.D.; Johir, M.A.H.; Hossen, J.; Rahman, M.S.; Zhou, J.L.; Hasan, A.T.M.K.; Karmakar, A.K.; Ahmed, M.B. The potentiality of rice husk-derived activated carbon: From synthesis to application. *Processes* **2020**, *8*, 203. [[CrossRef](#)]
23. Chafidz, A.; Astuti, W.; Hartanto, D.; Mutia, A.S.; Sari, P.R. Preparation of activated carbon from banana peel waste for reducing air pollutant from motorcycle muffler. *MATEC Web Conf.* **2018**, *154*, 01021. [[CrossRef](#)]
24. Da Costa, W.K.O.C.; Gavazza, S.; Duarte, M.M.M.B.; Freitas, S.K.B.; de Paula, N.T.G.; Paim, A.P.S. Preparation of Activated Carbon from Sugarcane Bagasse and Removal of Color and Organic Matter from Real Textile Wastewater. *Water Air Soil Pollut.* **2021**, *232*, 358. [[CrossRef](#)]
25. Kakom, S.M.; Abdelmonem, N.M.; Ismail, I.M.; Refaat, A.A. Activated Carbon from Sugarcane Bagasse Pyrolysis for Heavy Metals Adsorption. *Sugar Tech* **2022**, *25*, 619–629. [[CrossRef](#)]
26. Kaushik, A.; Basu, S.; Singh, K.; Batra, V.S.; Balakrishnan, M. Activated carbon from sugarcane bagasse ash for melanoidins recovery. *J. Environ. Manag.* **2017**, *200*, 29–34. [[CrossRef](#)]
27. Bachrun, S.; Ayurizka, N.; Annisa, S.; Arif, H. Preparation and characterization of activated carbon from sugarcane bagasse by physical activation with CO₂ gas. *IOP Conf. Ser. Mater. Sci. Eng.* **2016**, *105*, 012027. [[CrossRef](#)]
28. Liu, Q.S.; Zheng, T.; Wang, P.; Guo, L. Preparation and characterization of activated carbon from bamboo by microwave-induced phosphoric acid activation. *Ind. Crops Prod.* **2010**, *31*, 233–238. [[CrossRef](#)]
29. Zanzi, R.A.; Petrov, N.; Budinova, T.; Razvigorova, M.; Minkova, V.; Zanzi, R.; Björnbo, E. Preparation of activated carbons from cherry stones, apricot stones and grape seeds for removal of metal ions from water. In Proceedings of the 2nd OlleIndstorm Symposium on Renewable energy-Bioenergy, Stockholm, Sweden, 1 July 1999.

30. Olivares-Marín, M.; Fernández-González, C.; Macías-García, A.; Gómez-Serrano, V. Preparation of activated carbon from cherry stones by chemical activation with $ZnCl_2$. *Appl. Surf. Sci.* **2006**, *252*, 5967–5971. [CrossRef]
31. Olivares-Marín, M.; Fernández-González, C.; Macías-García, A.; Gómez-Serrano, V. Porous structure of activated carbon prepared from cherry stones by chemical activation with phosphoric acid. *Energy Fuels* **2007**, *21*, 2942–2949. [CrossRef]
32. Sultana, M.; Rownok, M.H.; Sabrin, M.; Rahaman, M.H.; Alam, S.M.N. A review on experimental chemically modified activated carbon to enhance dye and heavy metals adsorption. *Clean. Eng. Technol.* **2022**, *6*, 100382. [CrossRef]
33. Chen, J.P.; Wu, S. Acid/Base-Treated Activated Carbons: Characterization of Functional Groups and Metal Adsorptive Properties. *Langmuir* **2004**, *20*, 2233–2242. [CrossRef] [PubMed]
34. Neme, I.; Gonfa, G.; Masi, C. Activated carbon from biomass precursors using phosphoric acid: A review. *Heliyon* **2022**, *8*, e11940. [CrossRef] [PubMed]
35. Pak, S.H.; Jeon, M.J.; Jeon, Y.W. Study of sulfuric acid treatment of activated carbon used to enhance mixed VOC removal. *Int. Biodeterior. Biodegrad.* **2016**, *113*, 195–200. [CrossRef]
36. Diao, Y.; Walawender, W.P.; Fan, L.T. Activated carbons prepared from phosphoric acid activation of grain sorghum. *Bioresour. Technol.* **2002**, *81*, 45–52. [CrossRef] [PubMed]
37. Wan Ibrahim, W.M.H.; Mohamad Amini, M.H.; Sulaiman, N.S.; Wan Abdul Kadir, W.R. Evaluation of alkaline-based activated carbon from *Leucaena Leucocephala* produced at different activation temperatures for cadmium adsorption. *Appl. Water Sci.* **2021**, *11*, 1. [CrossRef]
38. Geng, Z.; Xiao, Q.; Lv, H.; Li, B.; Wu, H.; Lu, Y.; Zhang, C. One-Step Synthesis of Microporous Carbon Monoliths Derived from Biomass with High Nitrogen Doping Content for Highly Selective CO_2 Capture. *Sci. Rep.* **2016**, *6*, 30049. [CrossRef]
39. Wojnicki, M. Kinetic studies of the sorption process of Pd(II) chloride complex ions from diluted aqua solutions using commercially available activated carbon. *React. Kinet. Mech. Catal.* **2017**, *122*, 177–192. [CrossRef]
40. Hanum, F.; Bani, O.; Wirani, L.I. Characterization of activated carbon from rice husk by HCl activation and its application for lead (Pb) removal in car battery wastewater. *IOP Conf. Ser. Mater. Sci. Eng.* **2017**, *180*, 012151. [CrossRef]
41. Askari, R.; Mohammadi, F.; Moharrami, A.; Afshin, S.; Rashtbari, Y.; Vosoughi, M.; Dargahi, A. Synthesis of activated carbon from cherry tree waste and its application in removing cationic red 14 dye from aqueous environments. *Appl. Water Sci.* **2023**, *13*, 90. [CrossRef]
42. Yılmaz, F.M.; Görgüç, A.; Karaaslan, M.; Vardin, H.; Ersus Bilek, S.; Uygün, Ö.; Bircan, C. Sour Cherry By-products: Compositions, Functional Properties and Recovery Potentials—A Review. *Crit. Rev. Food Sci. Nutr.* **2019**, *59*, 3549–3563. [CrossRef]
43. Food and Agriculture Organization of the United Nations. Crops and Livestock Products. Available online: <https://www.fao.org/faostat/en/#data/QCL> (accessed on 11 March 2023).
44. Wojnicki, M.; Socha, R.P.; Pędzich, Z.; Mech, K.; Tokarski, T.; Fitzner, K. Palladium(II) Chloride Complex Ion Recovery from Aqueous Solutions Using Adsorption on Activated Carbon. *J. Chem. Eng. Data* **2018**, *63*, 702–711. [CrossRef]
45. Saad, E.; Mostafa, M. Pyrolysis characteristics and kinetics parameters determination of biomass fuel powders by differential thermal gravi-metric analysis tga/dtg. *Energy Convers. Manag.* **2014**, *85*, 165. [CrossRef]
46. Buettner, L.C.; Leduc, C.A.; Glover, T.G. Instantaneous ignition of activated carbon. *Ind. Eng. Chem. Res.* **2014**, *53*, 15793–15797. [CrossRef]
47. Du, J.; Dou, B.; Zhang, H.; Wu, K.; Gao, D.; Wang, Y.; Chen, H.; Xu, Y. Non-isothermal kinetics of biomass waste pyrolysis by TG-MS/DSC. *Carbon Capture Sci. Technol.* **2023**, *6*, 100097. [CrossRef]
48. Abbas, Q.; Mirzaei, M.; Ogwu, A.A.; Mazur, M.; Gibson, D. Effect of physical activation/surface functional groups on wettability and electrochemical performance of carbon/activated carbon aerogels based electrode materials for electrochemical capacitors. *Int. J. Hydrogen Energy* **2020**, *45*, 13586–13595. [CrossRef]
49. Yang, X.; Wan, Y.; Zheng, Y.; He, F.; Yu, Z.; Huang, J.; Wang, H.; Ok, Y.S.; Jiang, Y.; Gao, B. Surface functional groups of carbon-based adsorbents and their roles in the removal of heavy metals from aqueous solutions: A critical review. *J. Chem. Eng.* **2019**, *366*, 608–621. [CrossRef] [PubMed]
50. Wojnicki, M.; Fitzner, K. Kinetic modeling of the adsorption process of Pd(II) complex ions onto activated carbon. *React. Kinet. Mech. Catal.* **2018**, *124*, 453–468. [CrossRef]
51. Mansour, A.T.; Alprol, A.E.; Abualnaja, K.M.; El-Beltagi, H.S.; Ramadan, K.M.A.; Ashour, M. Dried Brown Seaweed's Phytoremediation Potential for Methylene Blue Dye Removal from Aquatic Environments. *Polymers* **2022**, *14*, 1375. [CrossRef]
52. Elaigwu, S.E.; Rocher, V.; Kyriakou, G.; Greenway, G.M. Removal of Pb^{2+} and Cd^{2+} from aqueous solution using chars from pyrolysis and microwave-assisted hydrothermal carbonization of *Prosopis africana* shell. *J. Ind. Eng. Chem.* **2014**, *20*, 3467–3473. [CrossRef]
53. Petrović, J.; Ercegović, M.; Simić, M.; Kalderis, D.; Koprivica, M.; Milojković, J.; Radulović, D. Novel Mg-doped pyro-hydrochars as methylene blue adsorbents: Adsorption behavior and mechanism. *J. Mol. Liq.* **2023**, *376*, 121424. [CrossRef]
54. Podborska, A.; Wojnicki, M. Spectroscopic and theoretical analysis of $Pd^{2+}-Cl^{-}-H_2O$ system. *J. Mol. Struct.* **2017**, *1128*, 117–122. [CrossRef]
55. Kasaini, H.; Goto, M.; Furusaki, S. Selective separation of Pd(II), Rh(III), and Ru(III) ions from a mixed chloride solution using activated carbon pellets. *Sep. Sci. Technol.* **2000**, *35*, 1307–1327. [CrossRef]

56. Sharififard, H.; Soleimani, M.; Ashtiani, F.Z. Evaluation of activated carbon and bio-polymer modified activated carbon performance for palladium and platinum removal. *J. Taiwan Inst. Chem. Eng.* **2012**, *43*, 696–703. [[CrossRef](#)]
57. Di Natale, F.; Orefice, M.; La Motta, F.; Erto, A.; Lancia, A. Unveiling the potentialities of activated carbon in recovering palladium from model leaching solutions. *Sep. Purif. Technol.* **2017**, *174*, 183–193. [[CrossRef](#)]

Disclaimer/Publisher's Note: The statements, opinions and data contained in all publications are solely those of the individual author(s) and contributor(s) and not of MDPI and/or the editor(s). MDPI and/or the editor(s) disclaim responsibility for any injury to people or property resulting from any ideas, methods, instructions or products referred to in the content.